Influence of Structural Features and Physico-chemical Properties of Metal-carbon Nanocomposites with Ferromagnetic Metal Inclusions on Microwave Radiation

L. Kozhitov[1], A. Kuzmenko[2], D. Muratov[1], V. Rodionov[2],
A. Popkova[1], E. Yakushko[1], M. Dobromyslov[3]

[1] *National University of Science and Technology "MISIS", 4, Leninsky Pr., Moscow, Russia*
[2] *South-West State University, 94, 50 Let Octyabrya Str., Kursk, Russia*
[3] *Pacific National University, 136, Tikhookeanskaya Str., Khabarovsk, Russia*

(Received 19 May 2014; published online 15 July 2014)

Metal-carbon nanocomposites on the basis of polyacrylonitrile and compounds of metals (Fe, Ni, Co) synthesized at IR-heating and studied by SEM, X-ray phase analysis, Raman scattering, IR Fourier spectroscopy are characterized by the carbon nanostructured amorphous graphite matrix with uniformly distributed nanoparticles of metals (10-30 nm), their oxides and compounds – $FeNi_3$ and FeCo, multilayered carbon nanotubes (~ 7-22 nm), and in the composition of Fe-Co / C fullerene-like formations – C_{60}. All nanocomposites feature high absorption of electromagnetic waves in the frequency range 20-40 GHz. Two absorption mechanisms are proposed: dielectric loss in the amorphous carbon matrix and scattering of electric and magnetic components by ferromagnetic inclusions. Absorption was – 8.68 dB for Fe-Ni / C, – 12.93 dB for Fe / C, and – 7.07 dB for Ni / C and for Fe-Co / C was found to be maximum in the whole range studied (more than – 40 dB) with a peak of – 52.83 dB at 24.27 GHz, which is explained probably by both high nanocomposite electric conductivity 2 S / m and high specific magnetization of phase FeCo.

Keywords: Polyacrylonitrile, IR-heating, Metal-carbon nanocomposites, Nanoparticles of metals, Carbon nanotubes, Ferromagnetic nanoparticles, Radiation-absorbing materials, Transmission coefficient, Reflection coefficient.

PACS numbers: 07.78. + s, 07.85.Fv, 42.65.Dr, 07.57. – c

1. INTRODUCTION

The extension of frequency range (up to tens of GHz) and the progress of wireless communication and microprocessor technology made the problem of protection of information systems from electromagnetic interference and an unauthorized access acute. Focus of investigations and the development of wideband absorbers of electromagnetic waves in the microwave region are mainly reflection and damping phenomena that are due to permittivity and permeability being complex and the change in media impedance [1]. The aim of those investigations is also the development of absorbing coatings with a clearly defined nanostructure [2-6] or composed of nanoparticles with high saturation thresholds for magnetization and permeability [7]. However, metal magnetic nanoparticles and absorbing nanostructured coatings do not secure in the wide Gigahertz range the reasonably stable attenuation coefficient since it turns out to be resonant-dependent on the coating thickness and/or domains that form nanostructures. Nanoencapsulated materials consisting of dielectric shells and magnetic nuclei that are characterized by an effective electromagnetic absorption [8-13] are being widely studied.

The present work deals with the carbon-ferromagnetic [14, 15] systems that have both high electroconductivity due to the extent of ordering of carbon structures and phases including carbon nanotubes (CNTs) and high values of magnetization for the saturation of electromagnetic phases whose complex permeability is slightly dependent on frequency because of eddy-current losses generated by an electromagnetic wave.

2. EXPERIMENTAL SECTION

Samples for study were metallocarbonic nanocomposites Fe-Ni / C – (1), Fe / C – (2), Ni / C – (3) and Fe-Co / C – (4) on the basis of polyacrylonitrile (PAN) [14, 15].

Table 1 – Initial parameters of precursors of nanocomposite synthesis

n/n	Nanocomposite	Initial composition	Metal concentration, %	Metal ratio	Synthesis temperature, °C
1	Fe-Ni / C	$FeCl_3$(hydr.)-$NiCl_2$(hydr.) / PAN	20	1÷1	500
2	Fe / C	$FeCl_3$(hydr.) / PAN	20	–	600
3	Ni / C	$NiCl_2$(hydr.) / PAN	20	–	500
4	FeCo / C	Fe(ac.ac.)-Co(ac.) / PAN	20	1÷1	800

Precursors for samples 1-3 were prepared by combined solution of PAN and chloride hydrate of a relevant metal in dimethyl formamide (DMFA) with a subsequent removal of the solvent. The concentration of PAN in the DMFA solution was 5 % and the metal 20 % of the polymer mass. Fe was introduced into sample 4 in the form of acetyl acetonate ($Fe(CH_3COCH = C(CH_3)O)_3$), cobalt – acetate ($Co(COOH)_2$). Pyrolysis was conducted in an IR-

The article was reported at the International Conference «The Advanced Technology, Equipment and Analytical Systems for Materials», Kursk, 13-14 May, 2014

heating chamber of installation "MILA-5000". The IR-heating was executed in a two-stage mode, namely, preliminary annealing in air at 150 and 200 °C for 15 min at each stage. In the heating process remains of the solvent bound with the polymer were removed and the initial cyclization and structurization of PAN occurred. The basic stage of IR-heating was carried out in vacuum (10-3 mm of mercury) at temperatures of 500-800 °C. The basic stage lasted for 15 min (Table 1) [14].

Morphological features and the changes in the surface structure of materials studied were investigated by using scanning electron microscope (SEM) JEOL JSM-6610LV (SEM, 20kV, up to 200000×). The distribution of chemical elements was determined with energy dispersive analyzer (EDA) Oxford Instrments X-Max Silicon Drift Detector 20 mm^2 with a resolving power of 0.1 μm. Phase analysis (PA) of samples was conducted with the use of powder diffractometer EMMA (60 kV, 80 mA,Cu Kα, 1.54 Å). The conductivity of samples as pressed tablets (250 atm, 1.1÷1.6 × 20 mm) was determined with LCR-meter Instek LCR-7821 with an alternating signal $U = 1$ B at a frequency $f = 1$ kHz. The complex reflection coefficient S11 and complex transmission coefficient S_{21} for all samples were measured with vector network analyzer Anritsu Wiltron 37369A in cavity resonator (28WCAK, КСВН = 1.30), which made it possible to discriminate and detect the levels of the incident and reflected electromagnetic waves penetrated through and reflected from a sample. Before the start of measuring screening characteristics the calibration of Anritsu Wiltron 37369A was done according to the standard procedure. The stacked powders under investigation filled tightly the resonator. For the frequency range of 20-40 GHz absolute values of frequency dependencies S_{21} (RL) and S_{11} were found as the voltage standing wave ratio (VSWR).

3. RESULTS AND DISCUSSION

According to scanning electron microscopy (SEM) and energy dispersive analysis (EDA) carbon particles have chiefly elongated shape the size of 0.5-1.0 μm, whereas the sphere-like formations, which, according to EDA, are metallic inclusions, have the size of 50 to 200 nm (Fig. 1, a-d).

Data of the elemental composition of samples 1-4 (Table 1) suggest that after thermal treatment the concentration of all powder samples is reduced from 20 % in the initial state to 16.4, 3.6, 5.5, and 3.1 %, respectively.

Table 2 – Energy dispersive analysis data

Sample	Element distribution, atomic mass					
	C	N	O	Fe	Co	Ni
1	50.2	19.9	13.6	8.6	0	7.8
2	63.9	20.4	12.1	3.6	0	0
3	65.3	22.3	7.0	0	0	5.5
4	96.9	0	0	1.5	1.6	0

X-ray phase analysis data are given as diffractograms (Figs. 2, a-d). For samples 1 and 4 the formation of diffraction maxima is observed at angles 2Θ = 26.6

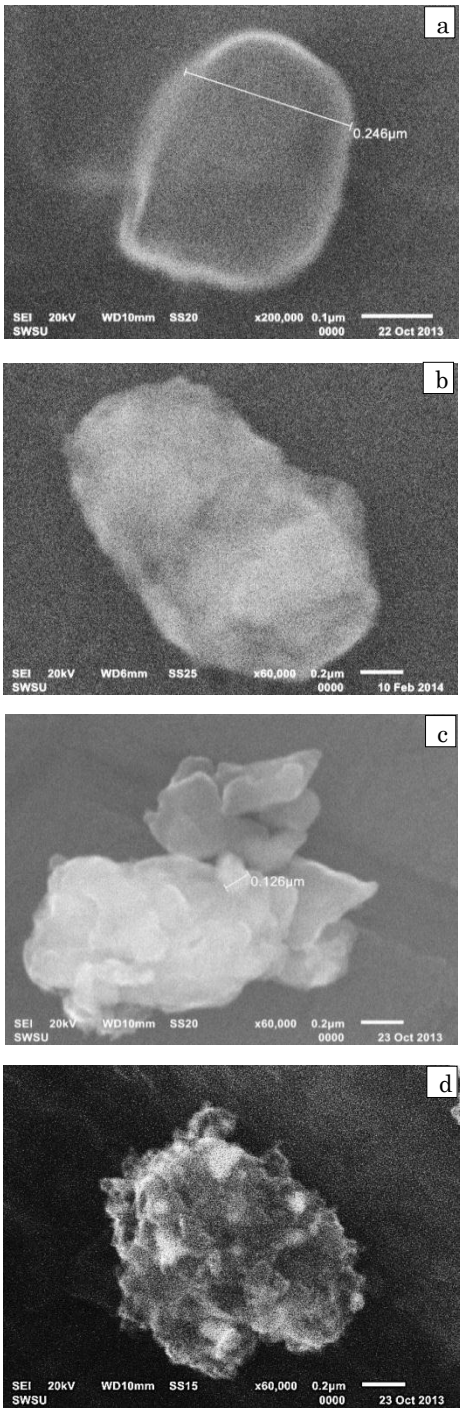

Fig. 1 – SEM images of carbon composites with inclusions of metal particles a) Fe-Ni; b) Fe; c) Ni; d) Fe-Co (60000× – 200000×)

and 26.2°, typical of hexagonal structure of graphite with an interlayer distance d equal to 3.40 Å and 3.35 Å from the planes (002) and (004), respectively, whereas for sample 3 in the range 15-30° data suggest the formation of amorphous halo. 2Θ = 43.32 and 2Θ = 44.76° in samples 2 and 3 correspond to cube lattices of iron (d = 2.01 Å) and nickel (d = 1.95Å), and reflections 2Θ = 33.0°, 35.7°, 37.1° and 44.9°, 45.0° – compounds of iron – Fe_2O_3 and FeC, and 2Θ = 37.0°, 43.1° and 44.9°, 45.1 – nickel – NiO and Ni_3C, respectively, which is in accord with data [2, 8].Maxima at

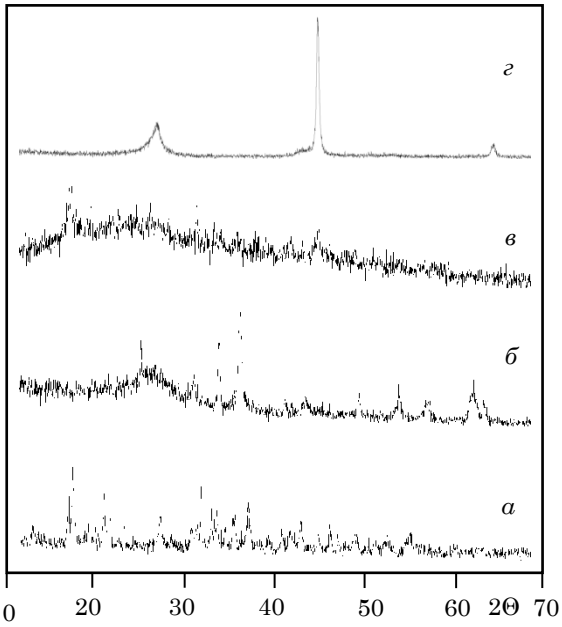

Fig. 2 – X-ray phase analysis of carbon composites (samples 1-4) with inclusion of metal particles a) Fe – Ni; b) Fe; c) Ni; d) Fe – Co

2Θ = 25.9°, 43.0° (Fig. 2c) correspond to planes (002) and (100) of hexagonal structure with parameters 3.53 Å and 2.26 Å, which is characteristic of materials with nanotubes and is probably due to the great number of free Ni atoms in the reaction chamber at IR-heating capable to cause the growth of nanotubes form gaseous carbon-bearing components [10]. Especially notable is the diffractogram for sample 4 which, besides the halo of carbon matrix with a maximum 2Θ = 26.6°, has lines 2Θ = 44.8° and a lower intensity 2Θ = 65.5°, that relevant to the volume-centered lattice of the compound iron-cobalt with inter layer distances of 2.01 Å and 1.42 Å from planes (110) and (200) [2, 3]. The halo at diffractograms of samples 1-3 indicates the high extent of matrix amorphism. At the same time, for sample 4 a clearer maximum is observed and the halo in noted for its lower fuzziness, which is indicative of the more ordered structure of the nanocomposite carbon matrix. With an increase in synthesis temperature of nanocomposites (800 °C) a clear crystal structure for alloy Fe-Co persists; in doing so, the intensity of the line corresponding to the carbon graphite-like matrix grows.

Data of X-ray phase analysis and SEM + EDA suggest that metal- carbon nanocomposites present nanoparticles either of metals (alloys) or oxides that are distributed in the carbon matrix with different amorphism, which is determined by both the conditions of the synthesis and the chemical composition of the metal component of the nanocomposite.

Features of the chemical structure of the carbon matrix, which presents the greater part of the nanocomposite, studied by Raman scattering (RS) are provided in Fig. 3. In all samples the origin of tangential vibrations of carbon atoms in the plane of graphite layer – G-band in the range 1500÷1600cm^{-1} occurred, which in some works is explained by the carbon nanotubes (CNTs) or similar carbon formations characterized by a dramatic bending of graphene planes [9, 10]. The extent to which the graphite structure is ordered is determined by the shape clearness and the intensity of G-band, which is typical of only sample 4. The intensity of excitations in D-band dominated in the range 1300÷1400 cm^{-1} at 1, 2, and 3 samples, which indicates a high imperfection of plane formations that is the extent of amorphization of the graphite layer due to a shift or a bending of carbon planes that consist of sp^2-hybridized carbon atoms. This is in accord with SEM data (Fig. 1). To characterize the extent to which carbon structures are ordered the ratio of band intensities I_D / I_G is used. Comparison of such quantities is given in Table 2, from which is seen that the greater ordering is for sample 4 (Fe-Co). For samples 1, 2, and 3 the expansion of G-band is observed due to the excitation of close in frequency vibrations. For example, for sample 3 – 1487, 1509, 1530 and 1576 cm^{-1}, difference of which makes it possible to evaluate the CNT diameter: $1 / \Delta\omega$ ~ from 6.6 to 22 nm. This degeneracy in the G-band form suggests multiple walls of CNTs and metal conductivity. All samples studied in low frequency range reveal radial vibrations of CNTs (RBM-band, insert in Fig. 3), being indicative of the existence of single-walled CNTs because radial vibrations of neighboring carbon atoms in multiple-walled CNTs are impossible. The CNT diameter is inversely proportional to frequencies in RBM-band [10].

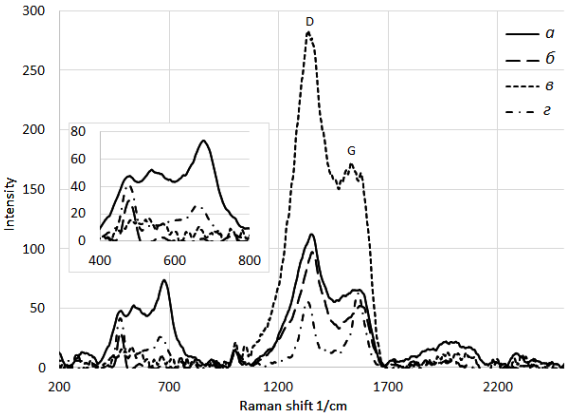

Fig. 3 – Raman scattering of carbon composites with inclusions of metal ferromagnetic particles: a) Fe – Ni; b) Fe; c) Ni; d) Fe – Co

For all samples in RBM-band a number of lines (three and more) are excited in the range 480÷672 cm^{-1}. Given that the minimum value found in expansion in G-band for sample 3 is 6.6 nm and inferences [10] ($\omega_{RBM} \sim A / d + B$, where A and B are empiric constants, a d is diameter of CNT) the CNT formation with d greater than 10 nm (insert in Fig. 3) can be expected.

Electric characteristics of the samples studied (resistivity, capacity, dielectric loss tangent and Q-factor) were studied with LCR-meter Instek LCR-819. Conductivity of samples 1, 2, and 3 turned out to be on the order of 1×10^{-6} Cm/m, that is close to dielectric value, whereas for sample 4 it was 2 Cm/m, close to metal value. This dramatic difference is due to both the extent of ordering of nanocomposite carbon matrix

Table 3 – Amorphization of sample predicted in G- and D-bands

Samples	G		D		Extent of amorphization
	Wave number, cm^{-1}	Intensity, rel.units	Wave number, cm^{-}	Intensity, rel. units	
1	1571.4	280.9	1356.6	323.1	1.15
2	1559.3	156.5	1359.6	203.7	1.30
3	1529.6	441.5	1344.4	538.8	1.22
4	1561.1	154.5	1329.9	146.5	0.95

and the absence of oxide forms of metal. Permittivity and permeability are complex: $\varepsilon^* = \varepsilon' - i\varepsilon''$ and $\mu^* = \mu' - i\mu''$, where the imaginary components are responsible for the efficiency of microwave absorption, and the real components cause the efficiency of electromagnetic energy transmission. In the coherent impedance mode (free space Z_0 (vacuum, air) and the external layer of the absorber Z_{abs} low reflection of electromagnetic waves occurs from the material surface. In this case, permittivity and permeability coincide $\varepsilon^* = \mu^*$ and in absolute value approach to unity. Pore or composite materials can meet the requirements. The reflection coefficient RL for them in the microwave band: $RL = 20\log|(Z_{abs.} - Z_0)/(Z_{abs} + Z_0)|$ [11], which allows one the creation from them screening coatings with high electric conductivity. It is natural that relaxation losses P_{rl} will be dictated by the dipole polarization of dielectric since the polarization rate P falls behind the variation rate of electric field E of radiation: $k_l a = ka(\mu\varepsilon)^{-1/2}$, where k_l and k are wave vectors, a is the radius of spherical surface, μ and ε are permeability and permittivity, respectively. The magnitude of loss is characterized by the work W_{rl} that is done by the alternating electric field to polarize the unit volume of dielectric: $P = \int(r - R)\rho d^3r$, where ρ is the electronic density, R is the particle radius. The magnitude of P, for example, for one Ni atom is small and amounts to 1.11×10^{-30} C × m [12]. However, the situation changes in going to nanosize domain and even more dramatically to cluster formations that appear in samples studied (Fig. 1). Given the really observed size of clusters (up to several μm) the value of P for agglomerates of metal particles can increase by several orders of magnitude. Critical becomes ferromagnetic nature of metal particles (Fe, Ni, Co) characterized by the excitation of surface Foucault currents, all the more so in microwave (MW) band due to skin-effect. The penetration depth of the MW radiation $\delta = (\pi f \xi \sigma)^{-1/2}$ [6], where f is the MW frequency, $\xi = \mu_0\mu^*$, σ is electroconductivity, can be calculated both taking into consideration the size of ferromagnetic nanoparticles [9] encapsulated in a carbon shell, which according to transmission electron microscopy is 10-50 nm. According to the SEM data the area occupies several hundredths nm (Fig. 1a, b). From this line of reasoning δ was evaluated to be 1 with values of permeability μ^* for a carbon shell, and for ferromagnetic particles 10^3; conductivity σ for carbon and particles amounted to 1 and 10^7 Cm/cm. Within the frequency range studied $f = 2 \times \div 4 \times 10^{10}$ Hz δ for the carbon shell was equal to 1 cm, and for the nucleus – 100 nm. Thus, scattering of microwave energy is of volume nature.

Figure 5 shows amplitude-frequency characteristic (AFC) of the transmission coefficient (S_{21}) for all samples studied obtained with Anritsu Wiltron 37369A. It is seen that the value of S_2 for samples with dielectric conductivity is reasonably low with peak values of 8.68 for sample 1, 12.93 for sample 2 and 7.07 dB for sample 3 in the frequency range 20-40 GHz. It should be noted that at absorption of 20 dB the microwave energy values decrease by 99 % [6]. Thus, values S_{21} found in samples 1-3 can be thought of as completely admissible. Sample 4, which featured quite good conductivity, has MW absorption characteristic of metals, namely, greater than – 40 dB in the whole region studied [1]. Therefore, S_{21} is dramatically. Qualitative explanation of features observed in spectra of MW absorption (Fig. 5) applied to samples 1-3 and sample 4 are likely due to different mechanisms.

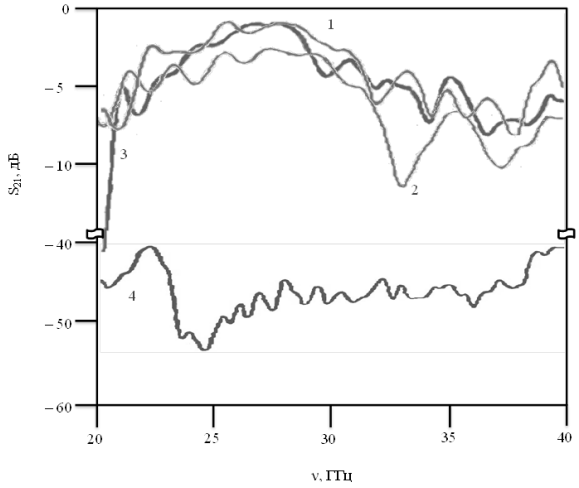

Fig. 5 – AFC of the transmission coefficient for carbon composites 1-4 with inclusion of metal particles: 1 – Fe / Ni; 2 – Fe; 3 – Ni; 4 – Fe / Co

For samples 1-3 MW absorption is dictated by both dielectric losses in heavily amorphous carbon matrix that contains products of PAN pyrolysis and the scattering of electric and magnetic components of the incident wave by ferromagnetic inclusions.

Intrinsic absorption by solid-phase polar complexes in the carbon matrix of nanocomposites at incident MW radiation, where ionization (energy was lower than $E_{ion.}$) and electron polarization (frequency was lower than 10^{13} Hz) were excluded, may be dictated by only resonant phenomena in the frequency range studied (20-40 GHz), which is corroborated by the form of the MW absorption spectrum (Fig. 5). According to IR-spectroscopy data obtained with IR Fourier spectrometer iS50 in the middle range in samples 1-3 absorption was observed at neighboring frequencies in the intervals 500÷800, 840÷1600, 1700÷2400 and 2900÷3600 cm^{-1}, which correspond to vibrations of CNTs and various complexes related to them [11]. Obviously, the intensity of excited eddy currents increases with conductivity growth as well as the magnitude of ponderomotive force in an alternating magnetic field of MW radiation $F = \mu_0\mu jH$, which causes elastic vibra-

tions in the system "nanocarbon structures-ferromagnetic nanoparticles" including CNTs, which are presumably revealed by Raman scattering (Fig.3) .Thus, the absorption in samples 1-3 can be dictated by resonant absorption by complexes [9] "carbon structures-ferromagnetic particles" when the frequency of their free oscillations ω_0 coincides with frequencies of MW radiation: $\omega_0 = (1 / 2\pi) (\gamma / m)$, where γ is rigidity, and m is CNT's mass.

MW absorption for sample 4 turned out to be maximum at a MW frequency of 24.27 GHz amounting to – 52.83 dB. Of note is the fact that this composite features conductivity typical of semiconductors (2 Cm/m). IR Fourier spectrum of sample 4 in any ways similar to the spectrum of C_{60} [9], and it has the most intensive absorption line: 530 cm^{-1}. The formation of fullerenes or similar structures at 800 °C is supported also by the relevant line 1460 cm^{-1} in the Raman scattering spectrum (Fig. 4). Thus, complex "carbon structures-ferromagnetic particles" in sample 4 can shield MW radiation. Considering that *specific magnetization of saturation* for the system of nanoparticles FeCo is 80 % higher than for FeNi: 210 and 120 Gs / g [4], respectively, hysteresis magnetic losses due to magnetization reversal in ferromagnetic inclusions must be added to eddy current losses.

4. CONCLUSIONS

Thus, it is shown that metal-carbon nanocomposites with ferromagnetic metal inclusions obtained at IR-heating are effective absorbers of electromagnetic radiation. It is found that addition of ferromagnetic nanoparticles to carbon nanostructures matrixes enhances the coefficient of MW absorption in all samples studied. MW absorption in practically meaningful dynamic range was found to be due probably to both the composition and structure of the carbon matrix and the inclusion of ferromagnetic nanoparticles.

REFERENCES

1. O.S. Ostrovsky, E.N. Odarenko, A.A. Shmatko, *Phys. Eng. Surface* **2**, 161 (2003) [In Russian].
2. Wei Lu, Ping Huang, Chenchong He, Biao Yan, *Int. J. Electrochem. Sci.* **8**, 914 (2013).
3. G.H. Lee, S.H. Huh, J.W. Jeong, et al., *J. Korean Phys. Soc.* **42**, 367 (2003).
4. V.F. Meshcheryakov, Y.K. Fetisov, et al., *J. Appl. Phys.* **104**, 063910 (2008).
5. H. Bayrakdar, *Prog. Electromagnet. Res.* **25**, 269 (2012).
6. Guo Jingbo, Duan Yuping, Liu Lidong, et al., *J. Electromagn. Anal. Appl.* **3**, 140 (2011).
7. S.J. Yan, L. Zhen, C.Y. Xu, *J. Magn. Magn. Mater.* **323**, 515 (2011).
8. Jiang Jingjing, Wang Han, Guo Huaihong, et al., *Nanoscale Res. Lett.* **7**, 238 (2012).
9. X.L. Dong, Z.D. Zhang, S.P. Jin, B.K. Kim, *J. Appl. Phys.* **86**, 6701 (1999).
10. V.G. Udovitsky, *Phys. Eng. Surface* No 4, 351 (2009).
11. U.J. Kim, X.M. Liu, C.A. Furtado, et al., *Phys. Rev. Lett.* **95**, 157402 (2005).
12. Z. Han, D. Li, H. Wang, et al., *Appl. Phys. Lett.* **95**, 023114 (2009).
13. M.V. Astakhov, V.A. Muratov, A.A. Frantsuzov, *J. Phys.: Condens. Matter.* **7**, 4565 (1995).
14. L.V. Kozhitov, A.P. Kuzmenko, S.L. Kozhitov, *J. Nano-Electron. Phys.* **5** No 4, 04007 (2013).